Available online at www.sciencedirect.com
SCIENCE DIRECT®
Journal of Power Sources 140 (2005) 59–65
JOURNAL OF POWER SOURCES
www.elsevier.com/locate/jpowsour

Development of nanophase CeO_2-Pt/C cathode catalyst for direct methanol fuel cell

Hwan Bae Yu[a], Joon-Hee Kim[a], Ho-In Lee[a,**], M. Aulice Scibioh[b], Jaeyoung Lee[b], Jonghee Han[b], Sung Pil Yoon[b], Heung Yong Ha[b,*]

[a] *School of Chemical Engineering and Research Center for Energy Conversion and Storage, Seoul National University, Seoul 151-744, South Korea*
[b] *Fuel Cell Research Center, Korea Institute of Science and Technology (KIST), Seoul 136-791, South Korea*

Received 23 July 2004; accepted 17 August 2004
Available online 13 October 2004

Abstract

Incorporation of nanophase ceria (CeO_2) into the cathode catalyst Pt/C increased the local oxygen concentration in an air atmosphere, leading to enhanced single-cell performance of direct methanol fuel cell (DMFC). Ceria doped catalysts were effective at low oxygen partial pressure ($\leq$0.6 atm) conditions and 1 wt.% CeO_2 doped Pt/C exhibited the highest performance. The effect of ceria was more prominent with air as the cathode reactant and the ceria acted as a mere impurity in a pure oxygen atmosphere, decreasing the DMFC performance. Impedance spectra showed a decrease in polarization resistance with the ceria addition to the cathode catalyst in low-potential regions confirming the facile mass transfer of the reactant oxygen molecules to catalytic sites. Transmission electron microscopy (TEM) pictures showed a uniform distribution of CeO_2 around platinum sites.

Keywords: Air utilization; Cathode catalyst; CeO_2; Direct methanol fuel cell; Oxygen storage material; MEA

1. Introduction

In spite of the fact that direct methanol fuel cell (DMFC) continues to trail the hydrogen–air polymer electrolyte membrane fuel cell (PEMFC) in power density, it does not require fuel processing equipment and hence avoids complex humidification and thermal management problems associated with PEMFC. The overall performance of DMFC depends on several factors, of which the most important are electrocatalytic activity of anode and cathode, ionic conductivity and resistance to methanol cross-over of the polymer electrolyte membrane and water management on the cathode side of the cell. Cathode research in DMFC technology is mainly focused on developing more selective and methanol-tolerant catalysts for oxygen reduction. In order to reduce the mixed potential due to methanol cross-over, the cathode catalyst should have a high exchange current density for oxygen reduction [1–5]. Increasing air utilization in the cathode is a direct methanol fuel cells is a viable proposition for portable power applications, since the burden of an air pump can be eliminated, thus reducing the volume, cost and energy consumption of the system. However, a fuel cell will exhibit lower performance when air is used instead of oxygen in the cathode compartment due to low partial pressure of oxygen in air at atmospheric pressure. Hence, the incorporation of oxygen storage material such as ceria (CeO_2) into cathode catalyst layer has been studied to increase the local oxygen concentration, leading to an enhancement of the fuel cell performance.

The ability of ceria to store, transport and release oxygen is of great importance in a range of clean-energy technologies [6–8]. CeO_2 has potential uses for the removal of soot

* Corresponding author. Tel.: +82 2 958 5275; fax: +82 2 958 5199.
** Co-corresponding author.
E-mail addresses: hilee@snu.ac.kr (H.-I. Lee), hyha@kist.re.kr (H.Y. Ha).

0378-7753/$ – see front matter © 2004 Elsevier B.V. All rights reserved.
doi:10.1016/j.jpowsour.2004.08.015

from diesel engine exhaust [9], for the removal of organics from wastewaters (catalytic wet oxidation) [10], as an additive for combustion catalysts and processes [11] and in fuel cell technology [12]. It forms an integral part of three-way catalysts and serves as a promoter in the commercial fluid catalytic cracking catalysts [13–15]. The excellent oxygen storage behavior of ceria is the result of a unique and delicate balance between structural (phase formation), kinetic (rate of shift between reduced and oxidized states: $Ce^{3+} \leftrightarrow Ce^{4+}$), and textural (presence of surface cerium sites) factors. The prime role of ceria is to maintain the local oxygen pressure by the reaction [16]:

$$CeO_2 \leftrightarrow CeO_{2-x} + \left(\frac{x}{2}\right) O_2 \qquad (0 \le x \le 0.5) \qquad (1)$$

Thus, ceria functions as an oxygen buffer. It is reasonable to expect that the incorporation of oxygen storage material into the catalyst layer of fuel cell cathode might lead to an increase in the local oxygen concentration. With this line of reasoning two reports were found in the literature, where vanadium oxide or zirconium doped CeO_2/Pt cathode catalysts led to performance improvements of PEMFC [17,18].

In this paper, we present our preliminary results on the effect of nanophase CeO_2 doped Pt/C cathode catalyst towards single cell performance of direct methanol fuel cell.

2. Experimental

2.1. Catalyst preparation and characterization

A ceria doped Pt/C catalyst was prepared by impregnating aqueous solution of $Ce(NO_3)_3{\cdot}6H_2O$ (CR-Kanto Chemicals Co. Inc., Japan) into 20–60% Pt/C catalysts (E-TEK). The resulting mixture was dried at 65 °C for 24 h and calcined at 300 °C for 2 h in nitrogen atmosphere to obtain CeO_2 doped Pt/C cathode catalyst of varied compositions, namely *x*C*y*P, where *x* is ratio of CeO_2 to platinum ($x = W_{CeO_2}/W_{Pt} \times 100$) and *y* is weight percent of platinum in Pt/C. The CeO_2 doped Pt/C was used as a cathode catalyst and Pt-Ru (50:50 atom%) black catalyst (Johnson Matthey, Inc.) was used as an anode catalyst.

The BET surface areas of the cathode catalyst samples were measured by N_2 adsorption using a Micromeritics ASAP2010 apparatus. X-ray diffraction (XRD) measurements were recorded on a Rint-Dmax 2500, Rigaku instrument, using a nickel-filtered Cu Kα (0.15418 nm) source. The average crystallite size was estimated with the help of the Debye–Scherrer equation, using the XRD data of all prominent lines. The morphologies of the catalysts were examined by transmission electron microscopic (TEM) technique using a Phillips - CM30 electron microscope.

2.2. Fabrication of the membrane electrode assembly (MEA)

Catalyst inks were prepared by mixing appropriate amounts of catalysts, deionized water, isopropyl alcohol (IPA), and 5% Nafion® solution (1100 EW, Du Pont). The amount of ionomer content was 15 wt.% to catalyst in the anode and 30 wt.% in the cathode, unless mentioned otherwise. A membrane-electrode assembly was fabricated by placing a Nafion® 115 membrane between a PtRu (3 mg cm^{-2}) anode and a Pt (3 mg cm^{-2}) (ceria doped and undoped) cathode followed by hot-pressing at 140 °C, 70 kg_f cm^{-2} for 150 s. An MEA for impedance analysis was fabricated with an undoped Pt electrode instead of a PtRu electrode.

2.3. Single-cell testing

All experiments including electrochemical measurements were conducted with cells, which consisted of MEAs sandwiched between two graphite flow field plates. The active area of the cell was 10 cm^2. In all the experiments operated in a fuel cell mode, 2 M methanol solution was pumped through the anode side at a flow rate of 5 mL min^{-1} and oxygen to the cathode side at a flow rate of 250 sccm or air (250 or 1250 sccm). The temperature and pressure of single cells were held at 80 °C and 1 atm, respectively. An oxygen or air stream to the cathode compartment was humidified by passing through a humidifier maintained at a temperature of 65 °C. Current–voltage curves were measured galvanostatically by using an electronic load (Daegil 500P).

2.4. Electrochemical measurements

Impedance spectra were obtained on MEAs as indicated below with a potentiostat (IM6, Zahner). The anode (Pt/C instead of PtRu/C, counter electrode) was supplied with a continuous stream of hydrogen (200 sccm) to make a dynamic hydrogen electrode (DHE) and to facilitate removal of permeated water at 80 °C and the cathode (Pt/C or Ceria-doped Pt/C) was supplied with a stream of humidified nitrogen (200 sccm) to form a working electrode (WE). All cathode impedance spectra reported here were measured between the cathode (WE) and the DHE in the complete fuel cell. The frequency range was chosen in the region from 50 MHz to 1 kHz and the amplitude of the sinusoidal current signal was adjusted so that the potential amplitude did not exceed 5 mV. The spectra were measured at dc potentials of 0.7, 0.8 and 0.9 V (versus DHE).

3. Results and discussion

In order to understand the performance enhancement in the presence of ceria as an oxygen storage material, single cell tests were made for direct methanol fuel cell with 20 wt.% Pt/C cathode catalyst in the presence and absence of 1 wt.% CeO_2 at a flow rate of 250 sccm pure oxygen, 250 and 1250 sccm air in the cathode compartment (Fig. 1). It can be seen that in an oxygen atmosphere the pure Pt/C

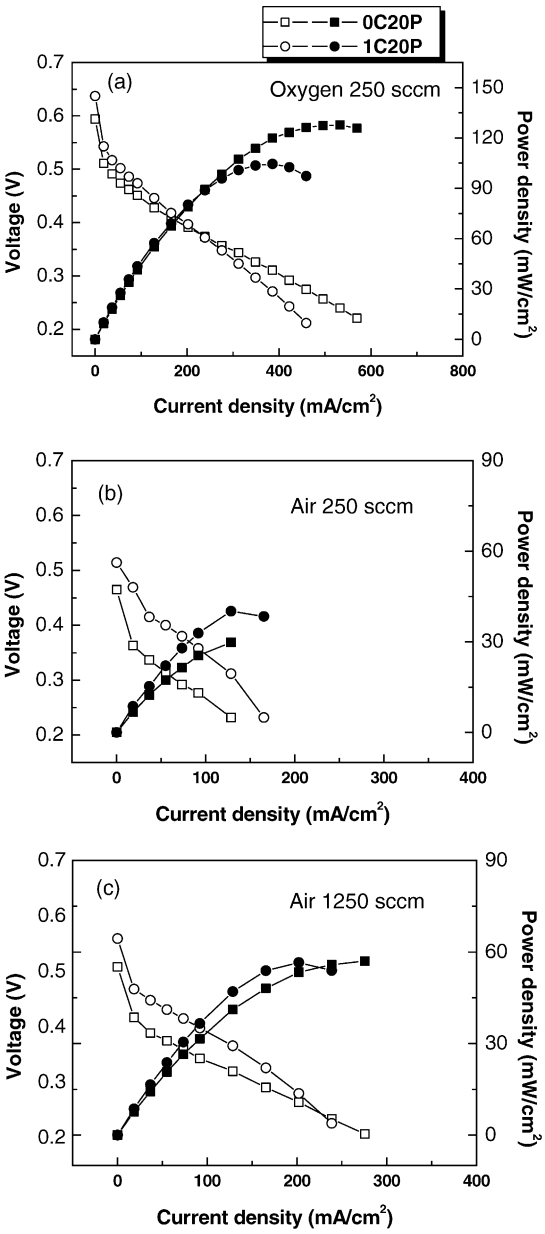

Fig. 1. Single cell performance of DMFC with 20 wt.% Pt/C catalyst in the presence and absence of CeO_2 under (a) oxygen 250 sccm, (b) air 250 sccm and (c) air 1250 sccm.

cathode catalyst exhibited a higher degree of performance (130 mW cm^{-2}) than ceria doped Pt/C (103 mW cm^{-2}) at 0.3 V (Fig. 1a). However, when air was used instead of oxygen, higher performances were noted for CeO_2 doped Pt/C in comparison to undoped Pt/C (Fig. 1b and c). Further, at low air flow rate (250 sccm) ceria exhibited pronounced effect because of oxygen deficiency in the catalyst layer (Fig. 1b); but at high air flow rate (1250 sccm), the mass transport of oxygen in the catalyst layer was accelerated and the ceria effect for enriching oxygen concentration was reduced (Fig. 1c). Even in the presence of oxygen storage material like ceria, the air had a much less performance than the pure oxygen because of large difference in oxygen partial pressure. Also, the performance was higher for air 1250 sccm than for air at 250 sccm. For instance, in the case of 1 wt.% of ceria doped Pt/C, the power density at 0.3 V was 103, 55 and 40 mW cm^{-2} for oxygen 250 sccm and air of 1250 and 250 sccm, respectively. Though the amount of oxygen availability is almost the same in the first two cases, the discrepancies in the performances are attributed to the fact that when air is used, there is nitrogen blanket formation in the cathode catalyst layer that hinders the accessibility of reactant oxygen molecules to the platinum catalytic sites [19].

In order to optimize the Pt content in the ceria doped Pt/C catalyst, single cell performances with different Pt/C catalysts were measured (Fig. 2a–c), while maintaining ceria content in the catalysts at 1 wt.%. It can be seen that 40 wt.% Pt/C exhibits the highest performance at all atmospheres regardless of the presence of ceria and the order of performance is: 1C40P > 1C60P > 1C20P. This observation may be ascribed

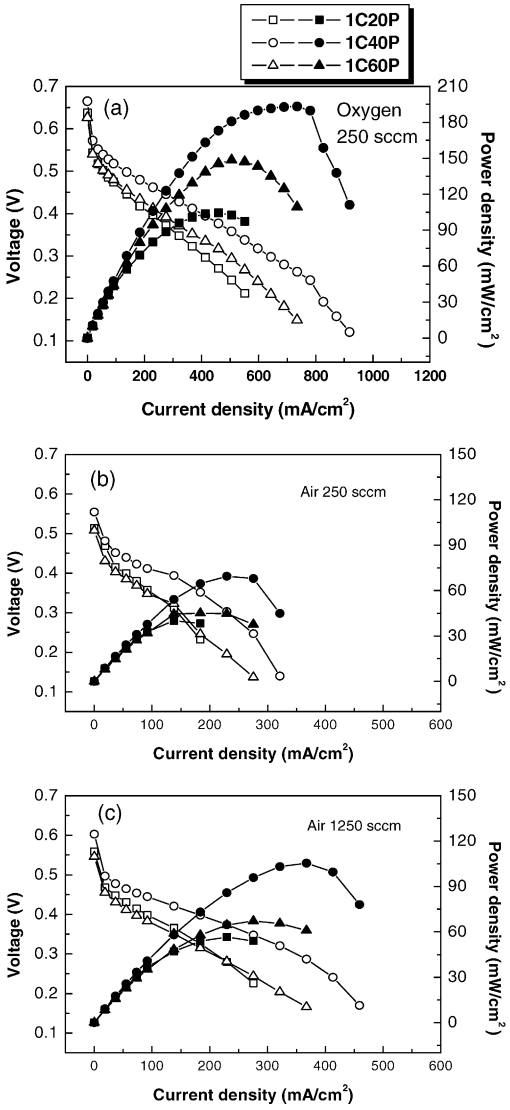

Fig. 2. Single cell performance of DMFC with 1 wt.% CeO_2 with different loadings of platinum under (a) oxygen 250 sccm, (b) air 250 sccm and (c) air 1250 sccm.

to the fact that the platinum particle size increased with increasing platinum content in the Pt/C catalyst, as reported in literature [20]. The average Pt particle sizes in 20, 40 and 60 wt.% Pt/C were 2.5, 3.9 and 8.8 nm, respectively, and the corresponding surface areas were 112, 72 and 32 m^2g^{-1} [21]. In case of 20 wt.% Pt/C, there was an increase in the relative number of edge atoms due to its small particulate size and the dispersion was higher than other loadings. However, this composition had a thicker catalyst layer compared to other catalyst loadings due to a higher amount of low-density carbon. A thicker catalyst layer hinders the facile mass transport of reactant gas molecules to the catalytic sites and increases the proton transport resistance in the catalyst layer. Hence the highest performance exhibited by 1C40P is attributed to the optimum availability of metal active surface area as well as the thickness of the catalyst layer.

To study the role of the oxygen storage ability of ceria, performance studies were conducted for various amounts of ceria incorporations under different cathode atmospheres, and the results are shown in Fig. 3a–c. In oxygen atmosphere, the pure Pt/C catalyst exhibited higher performance than the ceria doped Pt/C. This is because the addition of catalytically inactive ceria to Pt/C might have decreased the surface area of the platinum particulates. But in air atmosphere (flow rate of 250 or 1250 sccm), the highest performances were noted for 1 wt.% CeO_2 doped Pt/C. This is owing to the oxygen storage capacity (OSC) of ceria and its ability to rapidly exchange oxygen to buffer oxygen partial pressure oscillations [22]. It can be noted that the effect of ceria in the lower air flow rate is much pronounced, to an extent of 100% (Fig. 3b), while at the higher air flow rates, the efficiency improvement is only 75% (Fig. 3c). For very low additions of ceria (<1 wt.%), the oxygen storage ability in this catalyst formulations are not pronounced, and on the other hand, higher addition of ceria (>1 wt.%) may add resistance to the catalyst layer and decrease the active surface area of platinum particulates, since ceria is a poor electronic conductor as well as inactive to the oxygen reduction reaction. Therefore, an optimum amount of loading should be chosen to increase the local oxygen concentration and hence, oxygen supply to platinum active sites without appreciably affecting the catalytic activity of Pt. So, it is a delicate balance between the availability of platinum surface area and the oxygen storage ability of ceria that contributes to the performance with an optimum content of ceria.

As one can see in Figs. 1–3, the performance with ceria-doped Pt/C catalysts were affected by oxygen concentration in the cathode stream, and therefore, the effect of oxygen concentration was investigated in more detail. Fig. 4 shows the plots of current density at a constant voltage of 0.4 V for various oxygen partial pressures for 0 and 1.0 wt.% CeO_2 doped 40 wt.% Pt/C. It is clearly shown that at low oxygen partial pressures (≤0.6 atm) the CeO_2-doped Pt/C exhibited better performance than the pure Pt/C catalyst, whereas at high partial pressures of oxygen (>0.6 atm) the pure Pt/C catalyst showed higher performance than the ceria doped catalyst.

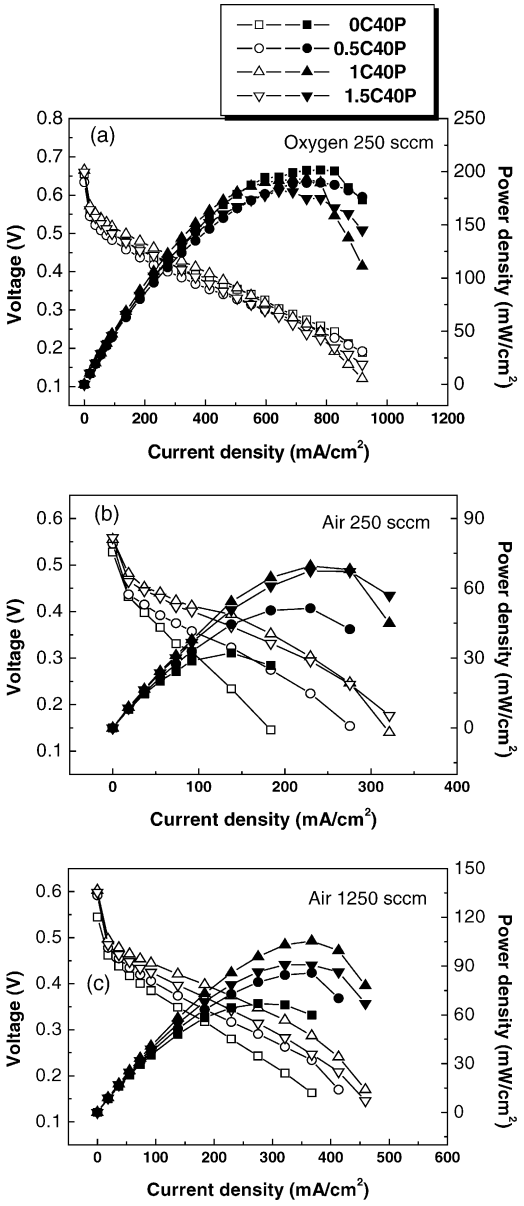

Fig. 3. Single cell performance of DMFC with 40 wt.% Pt/C catalyst with different loadings of CeO_2 under (a) oxygen 250 sccm, (b) air 250 sccm and (c) air 1250 sccm.

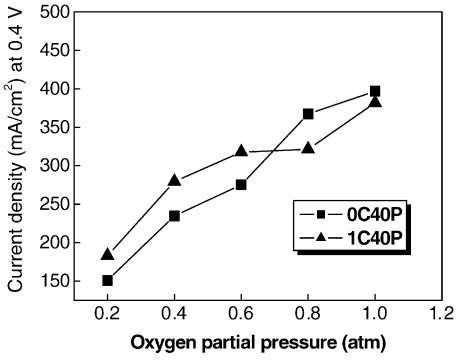

Fig. 4. Current density at a voltage of 0.4 V for different oxygen partial pressures (total flow rate: 250 sccm fixed).

All the above single cell performance studies of direct methanol fuel cell indicate that the ceria doped cathode catalyst exhibits better performance especially at low oxygen partial pressures in the cathode compartment and, on the other hand, the pure Pt/C catalyst is the best candidate in pure oxygen atmospheres. This can be confirmed further from the results of impedance studies that were carried out for the pure and ceria doped catalysts in air atmosphere at potentials from 0.7 to 0.9 V, and the corresponding Nyquist plots are shown in Fig. 5. In the spectra the diameter of arc is a measure of polarization resistance and the CeO_2 doped catalyst exhibits smaller resistances than the pure Pt/C at all potentials. The corresponding percentage decrease in polarization

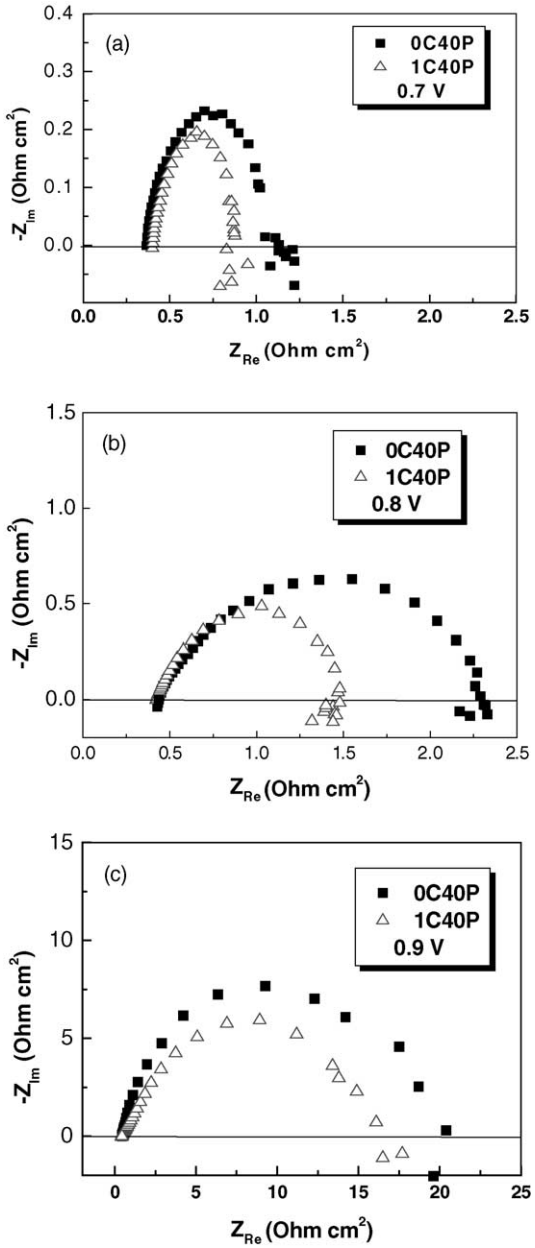

Fig. 5. Impedance spectra of the cathode with 0C40P and 1C40P in air at different potentials.

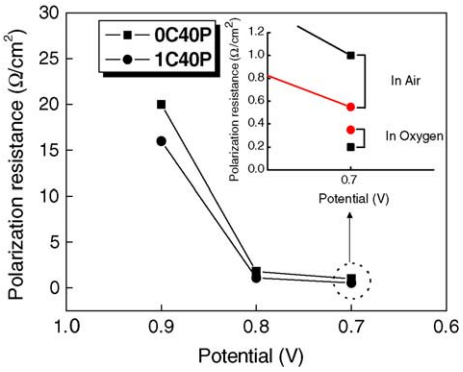

Fig. 6. Polarization resistance of the cathode in air at different potentials [Inset diagram compares the polarization resistance of the cathode in oxygen and air at 0.7 V].

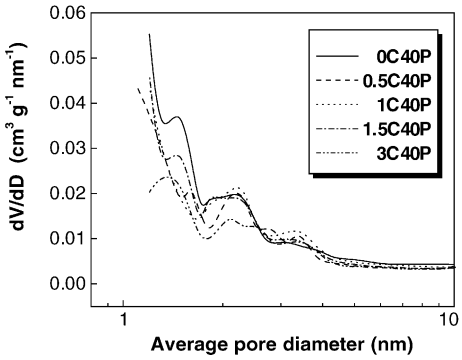

Fig. 7. Pore size distribution of 40 wt.% Pt/C catalyst with different loadings of CeO_2.

resistances by the addition of ceria are 20, 40 and 57% for potentials at 0.9, 0.8 and 0.7 V, respectively. Polarization resistance observed at a low-potential or at high current density is generally related to the mass transfer process because at low potentials the reaction rate is very high and thus oxygen depletion could occur to retard the reaction [23]. Therefore, the significant decrease in resistance noted at the low potential (0.7 V) may be attributed to more facile mass transfer of

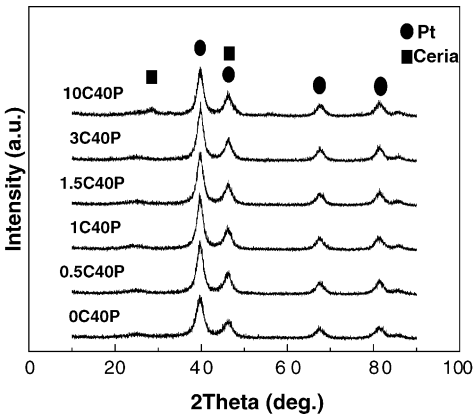

Fig. 8. XRD patterns of 40 wt.% Pt/C catalysts with different loadings of CeO_2.

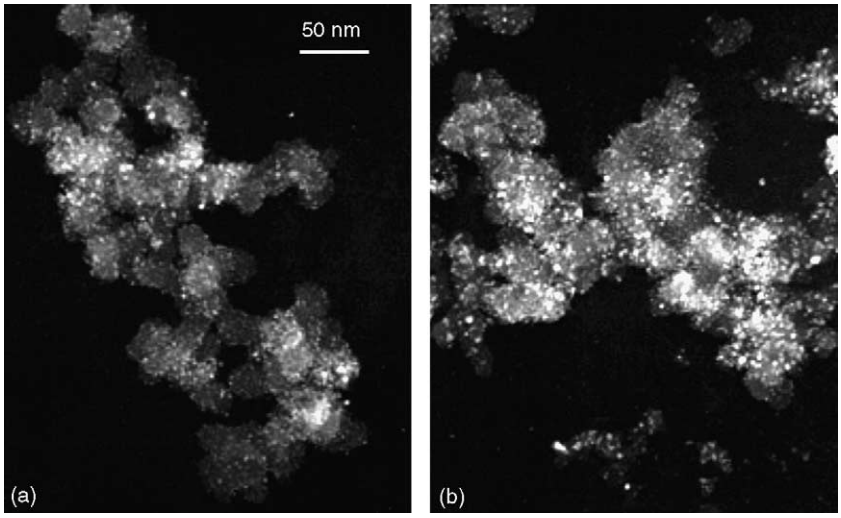

Fig. 9. TEM images of (a) 0C40P and (b) 1C40P.

oxygen molecules to Pt active sites for the ceria doped Pt/C catalyst.

Similar impedance studies were carried out in an oxygen atmosphere and Fig. 6 consolidates the polarization resistance of oxygen and air atmospheres at different potentials. As shown in the inset of the Fig. 6, in pure oxygen environment the Pt/C catalyst had lower resistance than the ceria doped Pt/C.

The microstructure evolution of the ceria catalyst was investigated using Brunauer-Emmett-Teller (BET) surface area and pore size distribution measurements, X-ray diffraction (XRD) and transmission electron microscopy (TEM) techniques.

Pore size distribution and BET surface area measurements were carried out for the 40 wt.% Pt/C with different content of ceria. Fig. 7 shows the pore size distribution of the selected catalyst samples. As the ceria content increased, appreciable decline in the pore volume was observed at the pores below 2 nm. And remarkable variation in pore size distribution was recorded for the 3.0 wt.% ceria content. The corresponding values of BET surface area of the samples are 122, 108, 117, 111 and 98 $m^2\,g^{-1}$ for the 0, 0.5, 1.0, 1.5, 3.0 wt.% CeO_2, respectively. The decrease in BET surface area of the Pt/C catalyst with the incorporation of ceria offers an evidence for its distribution throughout the catalyst textures and it also indicates that the platinum active sites could be blocked by ceria, leading to a reduced performance.

The X-ray diffraction patterns of ceria doped 40 wt.% Pt/C are shown in Fig. 8. The characteristic diffraction peaks of the face centered cubic crystalline (*fcc*) Pt, namely (1 1 1), (2 0 0), (2 2 0), (3 1 1) and (2 2 2) in the regions of 39.76, 46.24, 67.45, 81.28 and 87.00 (2θ) demonstrate the presence of Pt in metallic form [24] and, importantly, the lack of sharp peak rules out the presence of a significant mass-fraction of much larger crystallites. From the extent of the line broadening of (1 1 1) at 2θ of 39.76°, the average crystallite size is estimated to be 3.5–4.0 nm with the use of Scherrer equation after background subtraction [25]. The peaks in the regions of 28.4 and 47.5 can be indexed for CeO_2 with fluorite structure. The diffraction peaks are very feeble and the first peak is pronounced only at the higher concentrations of ceria incorporation; however the second peak is merged with the Pt (2 0 0) peak and this can be confirmed from increase in the heights of these peaks with increasing ceria content. However, there is no shift in any of the diffraction peaks of platinum metal at all compositions indicating that the added CeO_2 is not playing any role in influencing the crystallographic orientations of platinum catalyst particles supported on carbon.

The transmission electron microscopy (TEM) photographs of undoped and 1 wt.% CeO_2-doped 40 wt.% Pt/C are shown in Fig. 9, exhibiting the morphology and dispersion of Pt and CeO_2-Pt on carbon. In these pictures, the semi-transparent clusters are the aggregates of carbon black particles, the white dots are the dispersed platinum particles and the much denser white particles are ceria. The platinum particle size distribution is uniform and no agglomerates of metal particles are observed in both cases. The presence of CeO_2 in the catalyst appears to have relatively little effect on the platinum particle size, with the average particle size being 3.5–4.0 nm in both doped and undoped samples.

These observations indicate that the electronic and morphological state of ceria doped platinum catalyst is similar to the pure Pt/C catalyst.

4. Conclusion

The incorporation of an oxygen storage material such as ceria (CeO_2) into the cathode catalyst has been shown to increase the local oxygen concentration in the air atmosphere, leading to an enhancement in the performance of a DMFC. The resistance of the ceria doped Pt/C electrode was smaller than the normal Pt/C electrode in air operation especially at low-potentials as found in the impedance spectra, indicating

the more facile mass transport of reactant oxygen molecules to reactive platinum sites on ceria addition. The 1 wt.% CeO_2 doped 40% Pt/C was found to be an optimum catalyst composition exhibiting the highest performance in an air atmosphere. Higher loadings of ceria resulted in adverse effects on cell performance by decreasing the active surface area of platinum catalyst particulates and by increasing resistance in the catalyst layer due to the catalytically inactive and electrically nonconductive properties of ceria. In the catalyst formulations, ceria retained its fluorite structure and it did not influence the crystallographic orientations of platinum sites or alter the electronic state of the metallic phase in the platinum catalyst supported on carbon.

Acknowledgments

One of the authors, M. Aulice Scibioh, thanks Korean Federation of Science and Technology Societies (KOFST) and Korea Science and Engineering Federation (KOSEF) for support and assistance through Brain Pool Program.

References

[1] S.C. Thomas, X. Ren, S. Gottesfeld, P. Zelenay, Electrochim. Acta 47 (2002) 3741.
[2] S.L. Gojkovic, S. Gupta, R.F. Savinell, J. Electroanal. Chem. 462 (1999) 63.
[3] T.J. Schmidt, U.A. Paulus, H.A. Gasteiger, J. Electrochem. Soc. 147 (2000) 2620.
[4] N. A-Vante, B. Schubert, H. Tributsch, Mater. Chem. Phys. 22 (1989) 281.
[5] R. Jiang, D. Chu, J. Electrochem. Soc. 147 (2000) 4605.
[6] A. Trovarelli, C. Leitenburg, M. Boaro, G. Dolcetti, Catal. Today 50 (1999) 353.
[7] S. Bernal, J. Kasper, A. Trovaralli, Catal. Today 50 (1999) 173.
[8] A. Trovarelli, M. Boaro, E. Rocchini, C. Leitenburg, G. Dolcetti, J. Alloys Compd. 323–324 (2001) 584.
[9] J. Lahaye, S. Boehm, P.H. Chambrion, P. Ehrburger, Combust. Flame 104 (1996) 199.
[10] Y.I. Matatov-Meytal, M. Sheintuch, Ind. Eng. Chem. Res. 37 (1998) 309.
[11] W. Liu, M. F-Stephanopoulos, J. Catal. 153 (1995) 317.
[12] M. Sahibzada, B.C.H. Steele, K. Zheng, R.A. Rudkin, I.S. Metcalfe, Catal. Today 38 (1997) 459.
[13] J. Kaspar, P. Fornasiero, M. Graziani, Catal. Today 50 (1999) 285.
[14] K.C. Taylor, in: J.R. Anderson, M. Boudart (Eds.), Catalysis-Science and Technology, Springer, Berlin, 1984 (Chapter 2).
[15] K.C. Taylor, Catal. Rev. -Sci. Eng. 35 (1993) 457.
[16] G. Balducci, M.S. Islam, J. Kaspar, P. Fornasiero, M. Graziani, Chem. Mater. 12 (2000) 677.
[17] K. Kuwaha, A. Matsuoka, Japan Patent No. 1998-55807, 1998.
[18] Z. Xu, Z. Qi, A. Kaufman, J. Power Sources 115 (2003) 40.
[19] G.J.K. Acres, J.C. Frost, G.A. Hards, R.J. Potter, T.R. Ralph, D. Thompsett, G.T. Burstein, G.J. Hutchings, Catal. Today 38 (1997) 393.
[20] M. Umeda, M. Kokubo, M. Mohamedi, I. Uchida, Electrochim. Acta 48 (2003) 1367.
[21] Product catalog of E-Tek: http://www.etek-inc.com/com_nmc.php.
[22] R.K. Herz, Ind. Eng. Chem. Prod. Res. Dev. 20 (1981) 451.
[23] A.J. Bard, L.R. Faulkner, Electrochemical Methods Fundamentals and Applications, second ed., John Wiley & Sons, New York, 2001.
[24] C. He, H.R. Kunz, J.M. Fenton, J. Electrochem. Soc. 144 (1997) 970.
[25] H.P. Klug, L.E. Alexander, Wiley, New York 1973, pp. 635– 687.